

Institution: USPTO || [Sign In as Member or Individual \(Non-member\)](#) || [Contact Subscription Administrator at this Site](#) || [FAQ](#)*The Journal of Immunology*, 2000, 165: 331-338.Copyright © 2000 by [The American Association of Immunologists](#)

# Dominant Epitopes and Allergic Cross-Reactivity: Complex Formation Between a Fab Fragment of a Monoclonal Murine IgG Antibody and the Major Allergen from Birch Pollen Bet v 1<sup>1</sup>

Osman Mirza<sup>\*,†</sup>, Anette Henriksen<sup>2,\*</sup>, Henrik Ipsen<sup>†</sup>, Jørgen N. Larsen<sup>†</sup>, Margit Wissenbach<sup>†</sup>, Michael D. Spangfort<sup>†</sup> and Michael Gajhede<sup>3,\*</sup>

\* Protein Structure Group, Department of Chemistry, University of Copenhagen, Copenhagen, Denmark; and <sup>†</sup> Biochemical Allergy Research, ALK-Abelló, Hørsholm, Denmark

## Abstract

The symptoms characteristic of allergic hypersensitivity are caused by the release of mediators, i.e., histamine, from effector cells such as basophils and mast cells. Allergens with more than one B cell epitope cross-link IgE Abs bound to high affinity FcεRI receptors on mast cell surfaces leading to aggregation and subsequent mediator release. Thus, allergen-Ab complexes play a crucial role in the cascade leading to the allergic response. We here report the structure of a 1:1 complex between the major birch pollen allergen Bet v 1 and the Fab fragment from a murine monoclonal IgG1 Ab, BV16, that has been solved to 2.9 Å resolution by x-ray diffraction. The mAb is shown to inhibit the binding of allergic patients' IgE to Bet v 1, and the allergen-IgG complex may therefore serve as a model for the study of allergen-IgE interactions relevant in allergy. The size of the BV16 epitope is 931 Å<sup>2</sup> as defined by the Bet v 1 Ab interaction surface. Molecular interactions predicted to occur in the interface are likewise in agreement with earlier observations on Ag-Ab complexes. The epitope is formed by amino acids that are conserved among major allergens from related species within the *Fagales* order. In combination with a surprisingly high inhibitory capacity of BV16 with respect to allergic patients' serum IgE binding to Bet v 1, these observations provide experimental support for the proposal of dominant IgE epitopes located in the conserved surface areas. This model will facilitate the development of new and safer vaccines for allergen immunotherapy in the form of mutated allergens.

- ▶ [Abstract of this Article](#)
- ▶ [Reprint \(PDF\) Version of this Article](#)
- ▶ Similar articles found in:
  - ▶ [The JI](#)
  - ▶ [PubMed](#)
- ▶ [PubMed Citation](#)
- ▶ Search Medline for articles by:
  - ▶ [Mirza, O.](#) || [Gajhede, M.](#)
- ▶ Alert me when:
  - ▶ [new articles cite this article](#)
- ▶ [Download to Citation Manager](#)

- ▲ [Top](#)
- [Abstract](#)
- ▼ [Introduction](#)
- ▼ [Materials and Methods](#)
- ▼ [Results and Discussion](#)
- ▼ [References](#)

## ► Introduction

- ▲ [Top](#)
- ▲ [Abstract](#)
- [Introduction](#)
- ▼ [Materials and Methods](#)
- ▼ [Results and Discussion](#)
- ▼ [References](#)

The human type 1 allergic response is characterized by the presence of allergen-specific serum IgE. Allergic reactions involve the stimulation of allergen-specific Th2 cells leading to the production of specific IgE. The allergic hypersensitivity reaction is triggered by allergens aggregating preformed IgE Abs bound to the  $\alpha$ -chain of the high affinity Fc $\epsilon$ RI receptor on mast cell surfaces (1). These events have recently been reviewed (2). There is no reason to believe that the molecular interaction between allergens and Abs is unique compared with other Ag-Ab interactions. Obviously, allergens must have at least two distinct and spatially separated Ab-binding epitopes to aggregate the Fc $\epsilon$ RI-IgE complexes and function as allergens. Detailed analysis of the structure of allergen-Ab complexes, however, is expected to yield results important for the design of new and safer vaccines for allergen immunotherapy.

A limited number of structures representing inhalant allergens are known. The structures available represent the major birch pollen allergen, Bet v 1 (3), the homologous house dust mite allergens Der f 2 (4) and Der p 2 (5), the grass pollen allergen Phl p 2 (6), a minor allergen, profilin, from birch (7), the bovine dander allergen, Bos d 2 (8), and the ragweed pollen allergen, Amb t 5 (9). In addition to these, the structures of bee venom phospholipase A<sub>2</sub> (6) and that of a major wasp venom allergen Ves v 5 has been solved (A. Henriksen et al., manuscript in preparation). Comparing these allergens and their structures, it is evident that allergenicity cannot be rationalized on the basis of either overall folding patterns or biologic function, and hence, any protein should be regarded a potential allergen.

Ab-binding epitopes are sections of the molecular surface of the Ag. Determining the three-dimensional structure of the Ag enables identification of solvent-exposed amino acids constituting the molecular surface. The molecular structure of Bet v 1 was recently solved (3) and data on the identity of surface-exposed amino acids was combined with data on conserved amino acids comparing 57 homologous sequences within the *Fagales*. By this methodology, three conserved patches large enough to accommodate Ab-binding epitopes was identified and proposed to account for the clinically observed cross-reactivity of birch pollen allergic patients toward alder, hazel, and hornbeam.

It is tempting to speculate that these conserved surface areas indeed represent major IgE-binding epitopes. Immune responses in general are characterized by specificity and memory. These features are conveyed by Ag-specific T and B cells. The affinities of Ag-specific Abs are increasing on repeated exposure to the Ag in a process known as Ab affinity maturation (10). The molecular mechanism being based on point mutations introduced in the genetic material encoding the complementarity-determining regions (CDRs).<sup>4</sup> The magnitude of an immune response, furthermore, is determined by the dose and frequency of exposure to the specific Ag. Because tree pollen-allergic patients experience sequential exposure to pollens from hazel, alder, and birch, in Scandinavia over a period of 4 mo, exposure to the conserved surface areas is higher than that of the variable surface areas. High affinity IgE Abs are therefore more likely to be directed to the conserved surface areas than to the variable areas.

We here report a more direct approach to B cell epitope mapping by structural determination of allergen-Ab complexes. This study represents the first analysis of an allergen-Fab complex crystal structure though many studies of Ag-Fab complexes have been analyzed. These include the complexes with HIV1 capsid protein P24 (11), lysozyme (12, 13, 14, 15), other Fabs (16), neuraminidase (17, 18, 19), staphylococcal nuclease (20), a phosphocarrier protein, (HPr) from *Escherichia coli* (21), and Lyme disease Ag outer surface protein A (22).

X-ray crystallography requires homogeneous reagents for growth of crystals and cannot be performed using polyclonal human serum IgE. In the present study, Fab fragments from monoclonal murine IgG1 (BV16) raised by immunization with purified Bet v 1 have been used as a model system, because monoclonal allergen-specific human IgE is difficult to obtain. The use of IgG instead of IgE in the study of Ag-Ab interaction is justified by the generally accepted mechanism of VDJ gene assembly during early B cell maturation (10), but the system studied remains a model.

The BV16 epitope maps to one of the conserved surface patches described earlier (3). Because BV16 partially inhibits the binding of human serum IgE to Bet v 1, the epitope defined by BV16 is partly or completely overlapping Bet v 1 epitopes recognized by human serum IgE originating from natural exposure. The structure of the Bet v 1-BV16 Fab complex presented here defines the structural basis of a major allergen epitope. The complex provides information about Ab specificity and cross-reactivity having important implications for the design of new and safer vaccines for allergen immunotherapy, e.g., based on reduction of IgE binding by site-directed mutagenesis.

## ► Materials and Methods

### Ags and Abs

Pollen extracts from alder (*Alnus glutinosa*), birch (*Betula verrucosa*), hazel (*Corylus avellana*), and hornbeam (*Carpinus betulus*), were prepared as previously described (23). Bev 1 was purified from pollen extract by size exclusion, ion exchange and chelate chromatography as described (25). Recombinant Bet v 1 was expressed in *E. coli* and purified as previously described (24). Polyclonal anti Bet v 1 rabbit Abs were raised as described (23).

Monoclonal hybridoma Abs were derived from BALB/c mice immunized i.p. with purified Bet v 1 in IFA. Spleen cells from responding mice were fused with X-63 Ag 8.6.5.3 myeloma cells. Hybridoma cell cultures were grown in DMEM containing 10% (v/v) FCS, and culture supernatants were analyzed by direct ELISA. Positive cultures were cloned and recloned by limiting dilution until all wells derived from single cells were positive. mAbs were produced in Ag-free media. The monoclonality, isotype, and concentration of Ab were determined by isoelectric focusing, immunodiffusion, and single radial immunodiffusion, respectively. Finally, mAb was purified and concentrated by affinity chromatography on protein A-Sepharose CL4B (Pharmacia) according to standard procedures.

- ▲ [Top](#)
- ▲ [Abstract](#)
- ▲ [Introduction](#)
- ▼ [Materials and Methods](#)
- ▼ [Results and Discussion](#)
- ▼ [References](#)

Tree pollen-allergic patients' serum pool was a mix of equal volumes of serum from 15 RAST class 2 or 3 birch pollen allergic individuals.

### Cloning and sequencing of *Fv* genes

cDNA encoding heavy and light chain variable domains of murine mAb BV16 was amplified by PCR (25), cloned in pPCR2.1 (Invitrogen, San Diego, CA) and sequenced according to standard procedures.

### Immunoblotting

SDS-PAGE was performed as described (37) using 16% polyacrylamide gels. The gel was subsequently electroblotted semidry to nitrocellulose, which was processed as described (37).

### IgE inhibition assay

The ability of Ab BV16 to inhibit the binding of serum IgE to recombinant Bet v 1 was estimated in an IgE inhibition assay using a serum pool derived from birch-allergic patients. Serum IgE was captured by incubation with anti-IgE coupled to paramagnetic particles. After washing and resuspension in buffer, the Ab preparation tested was added followed by addition of biotinylated Bet v 1. The amount of biotinylated Bet v 1 bound to immobilized serum IgE was determined from the relative light units (RLU) measured after incubation with acridinium ester-labeled streptavidin. The degree of inhibition was calculated as  $(RLU_{\text{buffer}} - RLU_{\text{inhibitor}})/RLU_{\text{buffer}}$  obtained using buffer and respective Abs as inhibitors.

### Crystallization of Bet v 1-BV16 Fab complex

Fab fragments were generated by pepsin cleavage, and crystals of the Bet v 1-BV16 Fab complex were produced as described elsewhere (26).

Data collection. Initially, a room temperature data set was collected. As can be seen from the data in Table I, only diffraction to 3.5 Å was obtained. Consequently, we tried to increase the diffraction limit by using synchrotron radiation and cryogenic techniques. In both cases, integration, reduction, and merging of the data were conducted using DENZO and SCALEPACK (27).

**View this table:**

[\[in this window\]](#)

[\[in a new window\]](#)

Table I. Data collection and refinement statistics

Room temperature experiment. Data were collected in-house using a Rigaku R-axis IIC image plate system with a Rigaku RU200 rotating anode (Rigaku, Tokyo, Japan). The system was equipped with a graphite monochromator and a 0.5-mm collimator. The crystal was rotated through 90 frames with an oscillation of 2 degrees, an exposure of 30 min/frame, and a crystal to detector distance of 110 mm. Only one crystal was used for data collection.

Cryogenic temperature experiment. Data were collected at 120K from a single crystal, at the MAX-lab synchrotron facility beamline I711 (University of Lund, Lund, Sweden). Because the precipitant solution was not suitable for cryoexperiments and the crystals were unstable in all of the tested cryoprotectants (glycerol, 2-methyl-2,4-pentanediol (MPD), glucose, isopropanol, PEG 600), 10% glycerol was added to the precipitant solution during crystal growth. This did not seem to have any effect on the crystallization of the complex, and significantly improved the crystal stability when subsequently transferring the crystals to a cryobuffer containing 30% glycerol and precipitant. Three data sets were collected from one crystal and subsequently merged together. Collecting data set 1, the crystal was rotated through 60 frames, with an oscillation of 3 degrees, 2 min of exposure per frame, and a crystal to detector distance of 300 mm. A number of overloads were recorded in the resolution region  $>3.5$  Å; these reflections were then collected (data set 2) by rotating the crystal through 90 frames with 5 s exposure and 2 degrees oscillation per frame. To further increase the completeness, data set 3 was collected with 2.5 min of exposure, 2 degree oscillation per frame, and a crystal to detector distance of 200 mm. As can be seen from Table I, the cell dimensions are different at the two temperatures. Either the presence of the glycerol in the crystallization solution has changed the packing in the crystal or the crystal has undergone a temperature-dependent phase transition.

### Molecular replacement

Room temperature experiment. Molecular replacement was performed using AMoRe (28). The structure of Bet v 1 (3) and a model of the Fab fragment were used as search probes. Because only the sequence of the  $V_H$ - $V_L$  domain of the Fab fragment of BV16 was known at this time, the remaining part of the Fab fragment was described as alanines. The BV16 model was made by assigning coordinates from a known IgG1 Fab structure (1mlb (29)), to the BV16-Fab/ala sequence, using BIOSYM's HOMOLOGY program. There is a 2-residue insert in the CDR H3 loop of the BV16 relative to the model. In this region, a loop that did not introduce any unfavorable intermolecular contacts was built.

Rotation searches was first done with the Bet v 1, the constant, and the variable domains of BV16. This search gave two solutions. The searches were done in the resolution range 10–4 Å. Searching for rotation solutions with the whole Fab fragment gave no results. The correlation coefficients were 20.8 and 16.9, significantly higher than the following peak at 10.4. Fixing one solution straightforwardly gave the relative translation of the other. Rigid body refinement of this model gave an *R* factor of 40% and correlation coefficient of 64.

Cryogenic temperature experiment. The partially refined complex from the room temperature experiment was used as a search model. Rotation and translation searches were made in the region 8–4 Å. The rotation search gave two solutions (giving the rotations of complexes 1 and 2 and complexes 3 and 4, respectively), with correlation coefficients of 44.9 and 39.1 with significant contrast to the third peak at 15.9. Thus, the unit cell contains four complexes. The translation solution was found in the same way as described under the room temperature molecular replacement. Complexes 1 and 2 are related by translation only, and so are complexes 3 and 4. The translation vectors are in both cases (0.0, 0.5, 0.5). This is in agreement with the Patterson map. In general, the relative positions of the complexes in the crystal differ only slightly.

## Model building and refinement

The following is based on the cryogenic temperature data only, because this data set had the highest resolution. The refinement of the structure was conducted using initially the X-PLOR 3.851 program (30), and in the later stages of refinement CNS (0.5  $\beta$  Version) (31). The molecular replacement solutions from AMoRe were subjected to rigid body refinement, refining all 12 polypeptide chains as individual groups. The program o was used for manual fitting (32). A combination of torsion angle and cartesian dynamics including minimization and simulated annealing procedures were applied using the Engh-Huber parameters (33); 5% of the data was used for cross-validation. For the following rounds of refinement, strict noncrystallographic symmetry (ncs) was used. Torsion angle slowcool protocol runs (starting from 3000 K) and grouped  $B$  factor refinement (one  $B$  factor per residue) followed. After convergence of the  $R_{\text{free}}$ , manual electron density fitting was performed followed by positional refinement and restrained individual  $B$  factor refinement. The  $R_{\text{free}}$  now converged at 35%. Inspection of the electron density revealed that two of the complexes returned good density overall, whereas one complex (complex 3) showed weak density in some light chain regions, and one complex (complex 4) in several Bet v 1 regions (see definitions below).

However, none of these regions was at the Bet v 1-BV16 Fab interface. This and the high  $R_{\text{free}}$  suggested that restrained ncs should be applied, and from this point restrained refinement was used. To determine the optimal ncs restraints, torsion angle refinement runs at a constant temperature of 2500 K were performed using different weights. Refinement cycles with high ncs weights and individual restrained  $B$  factor refinement without ncs restraints gave the lowest  $R$  values, an  $R_{\text{free}}$  of 32.4% and a conventional  $R$  factor of 26.6%.

Inspection of the electron density revealed that the less well-defined parts of the structure still showed weak electron density. No clear results were obtained by calculating omit maps with the suspicious regions omitted. At this stage, the maximum likelihood target function in CNS was applied. The final structure of the X-PLOR refinement was subjected to a 5000 K slowcool run, using torsion angle dynamics, followed by  $B$  factor refinement. This immediately dropped the  $R_{\text{free}}$  to 30.4% and  $R$  value to 26.6%. Subsequent refinement cycles consisting of manual rebuilding, standard slowcool protocols from starting temperatures of 1500 and 700 K, initially with the maximum likelihood target function and ending with two rounds of refinement with the residual target function, giving the final  $R_{\text{free}}$  of 28.5% and  $R$  factor of 25.3%. The reason why strict ncs was not applied although very high restraint weights (3000 kcal/ $\text{\AA}^2$ ) were used was that refining the  $B$  factors without ncs constraints dropped the  $R_{\text{free}}$  ~ 1.2%.

Overall, the four complexes showed good density throughout the structure. The regions with weak electron density were loop 58–65 and loop 197–204 in the light chain, both showing poor side chain density. In the heavy chain, the loop 131–141 showed poor density, with density gaps in the main chain. Attempts to find alternative conformation with omit maps did not give unambiguous results. Previously, this region has been reported to be disordered (34). All N-terminals parts of the Fab molecules are well ordered, whereas the BV16 C-terminals could not be fitted properly. Additionally, the loops 60–65,

94–97, and 122–129 and residues 1–7, 36–40, and 155–157 showed weak density in one of the four bet v 1s. In one light chain, the loops 125–133, 167–174, and 180–187 and residues 11–16, 22–27, and 138–145 showed weak side chain density. Because none of these regions is problematic in the room temperature structure, these problems are attributed to static disorder as a consequence of the phase transition.

In the Bet v 1 molecules, D93 lies outside the allowed Ramachadran regions, which was also the case in the structure of native Bet v 1. Two residues from the light chain are in the disallowed regions, these are residues L30 and L68, both located in loop regions, with relatively well-defined density. In the heavy chain residue, H54 falls in the disallowed regions; again good density supports the conformation. Refinement statistics were calculated using CNS and PROCHECK (35)

The mean  $B$  values for complexes 1 and 2 are 54.1 and 57.8 Å<sup>2</sup>, and for complexes 3 and 4, they are 76.1 and 71.7 Å<sup>2</sup>. One of the complex molecules with the higher mean  $B$  value includes the bet v 1 with poor density, and the other includes the light chain with poor density. The clear difference in mean  $B$  values of the two pairs is probably due to the mentioned static disorder in the crystal and is an effect of the cryocooling.

## ► Results and Discussion

### Characterization of murine monoclonal BV16 Ab

A panel of murine mAbs was obtained after immunization with Bet v 1 purified from a birch pollen extract. Screening of the hybridoma candidates aimed at obtaining both Bet v 1 specific as well as Abs cross-reactive between the homologous major allergens from alder and hazel. For this purpose, all hybridomas were screened in direct ELISA using alder, birch, and hazel pollen extract, respectively. BV16 was selected as a cross-reactive Ab, subsequently confirmed by immunoblotting using pollen extracts from the *Fagales* species birch, hazel, alder, hornbeam, and recombinant Bet v 1 (Fig. 1□). Weak reactivity with the hazel major allergen is often encountered in this experimental setup. However, the reactivity with the major hazel allergen is comparable with that of the homologous major allergens. The result is most likely due to incomplete re-folding of the hazel allergen after denaturing electrophoresis as indicated by Ipsen and Larsen (36).

- ▲ [Top](#)
- ▲ [Abstract](#)
- ▲ [Introduction](#)
- ▲ [Materials and Methods](#)
- [Results and Discussion](#)
- ▼ [References](#)

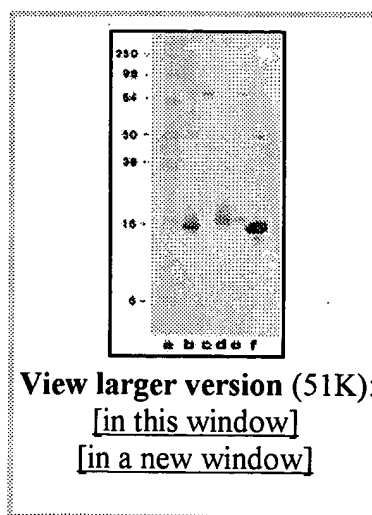


**FIGURE 1.** Immunoblotting of mAb BV16. Lane a, m.w. standards (kDa). Lanes b–e, pollen extracts from birch (lane b), hazel (lane c), alder (lane d), and hornbeam (lane e). Lane f, Recombinant Bet v 1.

The ability of Bet v 1-specific rabbit polyclonal and murine mAb BV16 to inhibit the binding of Bet v 1 to specific serum IgE derived from birch-allergic patients was addressed in an IgE inhibition assay (Fig. 2a). The Bet v 1-specific rabbit Abs were raised by repeated immunization using Bet v 1 purified from a pollen extract in IFA. By this procedure, the Ag will be partly denatured, and the resulting Ab will contain specificities directed at any conformation of the Ag. As a consequence, these Abs showed 100% inhibition in agreement with the notion that epitopes recognized by human-specific serum IgE are predominantly conformational and thus constitute only a fraction of those defined by the rabbit antiserum. Surprisingly, the mAb BV16 was able to inhibit ~40% (relative to the polyclonal rabbit Ab) of the binding of specific serum IgE to Bet v 1. This high proportion of inhibition not only shows that the surface area defined by the BV16 epitope is relevant also in terms of IgE specificities but also supports the concept of dominating IgE epitopes. Because the BV16 epitope is located in one of the conserved surface patches described earlier (3), it furthermore supports the notion that conserved surface areas constitute dominant epitopes for high affinity IgE.

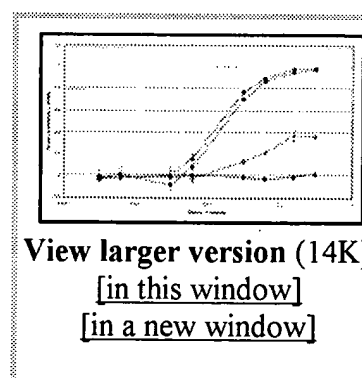


**FIGURE 2.** Serum IgE inhibition assay. Inhibition of the binding of biotinylated Bet v 1 to a pool of birch pollen-allergic patients' serum IgE by Ab preparations. ♦, Rabbit polyclonal anti-crude birch pollen extract; ■, rabbit polyclonal anti-Bet v 1 (X) murine monoclonal BV16; ▲, rabbit polyclonal anti-crude house dust mite extract. CL is confidence limits.

### Structural analysis of complex

The allergen Bet v 1 forms a 1:1 complex with BV16 Fab. The main structural feature of the allergen Bet v 1 is a seven-stranded anti-parallel  $\beta$  sheet that wraps around a 25-residue-long C-terminal amphipathic  $\alpha$  helix. The  $\beta$  sheet and the C-terminal part of the long helix are separated by two consecutive helices.



Between the two helices and the  $\beta$  sheet, there is a larger cavity and a forked tunnel through the structure.

Numerous structural studies have been performed on Abs including structure determinations of intact IgG Abs (37). There has been special focus on determining the regions involved in the interactions with Ag, the CDRs (38). All BV16 Fab CDRs except L2 are in proximity to Bet v 1. L2 can be seen on Fig. 3 in front of the 3 BV16 Fab strands most to the right, far from the complex interface. Interestingly, superposition of the template CDRs (9) and the corresponding BV16 Fab CDRs shows good agreement in conformation for the loops L1, H1, and H2 but not for L2. This probably reflects that the template CDR conformations are derived from CDRs that actually are in contact with the Ag, and not from loops that do not interact. In previous investigations of Fab-Ag complexes, it is frequently seen that there are CDRs not involved in the complex formation.

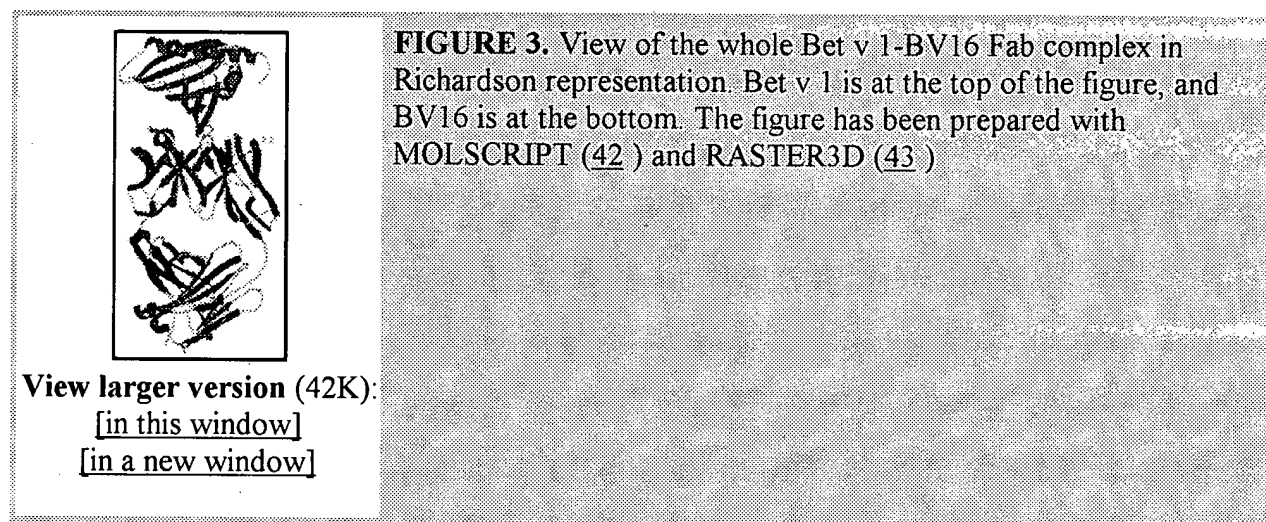


Fig. 3 shows an overall view of the complex between Bet v 1 and BV16 Fab. No major conformational changes in the structure of Bet v 1 are seen upon binding to the monoclonal BV16 Fab. The overall rms deviation between free and bound Bet v 1 is 0.605 Å, as calculated by the program o (39).

Fig. 4 shows the contact surfaces found on BV16 and Bet v 1, respectively. Contacts are defined as the molecular surfaces of the two molecules that are <3.2 Å apart. The calculation of the contact surfaces was performed with the program GRASP (40). The buried area on Bet v 1 is calculated to be 931 Å<sup>2</sup> (of a total molecular surface of 9,119 Å<sup>2</sup>) and the buried area on BV16 Fab is 807 Å<sup>2</sup> (of 21,648 Å<sup>2</sup>). This is comparable to what is found for other protein-Fab complexes (41). For example, the buried area is reported to be 916 Å<sup>2</sup> in the influenza virus N9 neuraminidase-NC41-Fab complex (19).



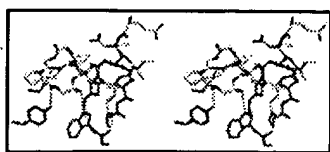
View larger version (125K):  
[\[in this window\]](#)  
[\[in a new window\]](#)

**FIGURE 4.** Contact surfaces of Bet v 1 and BV16 colored after electrostatic potential. Ribbon diagram of Bet v 1 and the variable domain of the BV16 Fab. Bet v 1 is at the top of the figure, and BV16 is at the bottom. In addition, the molecular surfaces of the interacting regions are shown. The surfaces are defined to include only the contributions of residues with a maximum intermolecular distance of 3.2 Å. The surfaces are colored according to the value of the electrostatic potential generated by the isolated proteins, with red representing -10 kT and blue representing 10 kT. For a better view of the charge and surface complementarity, the  $F_V$  has been tilted ~70 degrees. The significant red bump on the Bet v 1 surface is the E45 (central in the p loop-containing 42–52 region); the corresponding interaction region is the blue hole in the BV16 Fab surface. This figure has been prepared with GRASP (44).

Given the small sizes of the epitope (only around 10% of the total allergen surface), it is obvious that it is theoretically possible to bind more than one IgE molecule to the same allergen molecule. Table II lists the intermolecular contacts between Bet v 1 and BV16 Fab with hydrogen bonds emphasized. One-half of the residues that constitute the epitope are involved in hydrogen bonds. This means that the interaction must be classified as a mixture of hydrogen bonding and van der Waals interactions. Bet v 1 has surface patches, which are either very hydrophobic or dominated by polar residues, but neither of these is part of the epitope mapped out by the BV16 Ab. Central hydrogen bonds in the interface are shown in Fig. 5. The epitope must be classified as discontinuous. However, residues 42–52 (including the alleged "p-loop like" region 46–51 of the Bet v 1 sequence constitute ~80% of the contact surface. A total of eight intermolecular hydrogen bonds are found in the complex; all of these are in the 42–52 region of Bet v 1. The contacts are to the L1, L3, H1, and H3 CDRs and the only residue without Fab contacts is G48. E45 is situated in the center of the epitope, forming two short hydrogen bonds to backbone nitrogen atoms of the Fab fragment H1 and H3 CDRs. It is an obvious candidate for site-directed mutagenesis studies aiming at altering the Ab-binding properties of Bet v 1. A close-up of the interaction region is shown in Fig. 6, including the calculated electron density when omitting this region from the Fourier synthesis. The other contacts to BV16 Fab are made by Bet v 1 residues R70, D72, H76, I86, E87, and K97. Although the continuous region 42–52 of Bet v 1 is participating in the majority of complex interactions, the Bet v 1-synthetic peptide 39–53 is not able to inhibit the binding of Bet v 1 to BV16 as judged by ELISA (data not shown). Thus, the constraints imposed by the structure of Bet v 1 on the conformation of loop 42–52 seem to be of major importance for Ab binding.

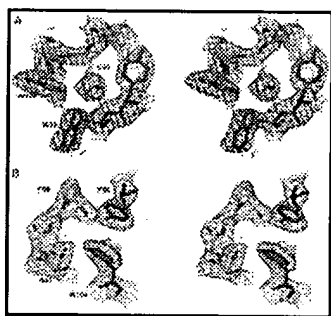
View this table:  
[\[in this window\]](#)  
[\[in a new window\]](#)

Table II. Contacts between Bet v 1 and BV16<sup>1</sup>



View larger version (21K):  
[\[in this window\]](#)  
[\[in a new window\]](#)

**FIGURE 5.** Close-ups of interaction region. Stereo view of the interactions involving all hydrogen bonds formed on complexation. Bet v 1 residues have yellow carbon atoms whereas BV16 Fab residues have green carbon atoms. Only Bet v 1 residues involved in hydrogen bonds are labeled. E45 makes two short hydrogen bonds with the BV16 backbone WH33 NH and GH99, both 2.9 Å. N47 is in position to make hydrogen bonds with SL91 (2.7 Å). In addition, the following hydrogen bonds are formed: N43 to DH102, G46 to TH103, P50 to YL96, and G51 to WH33. This figure has been prepared with MOLSCRIPT and RASTER3D.



View larger version (90K):  
[\[in this window\]](#)  
[\[in a new window\]](#)

**FIGURE 6.** Omit maps of the major interaction region. This figures show stereo views of an omit map of the major Bet v 1-BV16 Fab interaction region contoured at 1.3  $\sigma$ . A, Bet v 1 residues G44, E45, I46, and BV16 Fab residues YH32, WH33, WH104. B, Bet v 1 residues N47, G48, G49, and P50 along with Fab residues WH104 and YL96. These figures have been prepared with DINO (<http://www.bioz.unibas.ch/~x-ray/dino>) and RASTER3D

A detailed analysis of Ab-Ag interactions has recently been undertaken (38). They have grouped the interactions based on the size of the Ag: small molecule (hapten) interactions; peptide interactions; and large (protein) interactions. When comparing the interactions seen with the normalized frequency of interaction for each amino acid in the CDRs, it is found that all interacting residues from BV16 Fab have frequencies above 0.2. None of the CDR residues described as "only structural" by MacCallum et al. interacts with the Bet v 1. They also note that large Ags seem to prefer contacts with residues at the extremities of the combining site, e.g., most of L2 and residues H30–H32 in H1. Although BV16 Fab has contacts to both H31 and H32, there are no contacts to L2. This is not uncommon. In the complex between hen egg lysozyme and the Fv fragment of its mAb D11.15 (14), neither L1 nor L2 interacts with the Ag.

Because the BV16 Ab cross-reacts with the major allergens from other trees of the *Fagales* order, BV16 is expected to bind to one of the patches of conserved residues on the molecular surface of Bet v 1 defined previously (3). Fig. 7 shows the epitope defined by the BV16 Ab and a corresponding molecular surface defined by the residues completely conserved among all *Fagales* major allergens (3). The surface area defined by the conserved residues is contained in the surface area defined by the interactions with BV16 Fab.



[View larger version \(44K\):](#)

[\[in this window\]](#)

[\[in a new window\]](#)

**FIGURE 7.** Bet v 1 epitope and patch of conserved residues in the *Fagales* order. The solvent-accessible surface of Bet v 1 is shown. The surface was calculated with a probe with radius of 1.4 Å. *A*, Patch of conserved residues among the allergens from the *Fagales* tree order (gray), comprising residues 41–52; *B*, gray areas, the residues comprising the BV16 epitope with the same orientation of the molecule. All except one Bet v 1 residue (residue 41) from the conserved patch are involved in contacts with the BV16 Fab. This explains why the BV16 is known to bind to allergens from pollen from other trees. The figure was prepared with SPOCK and RASTER3D.

In conclusion, the interactions observed in the Bet v 1-BV16 Fab complex can be described in terms of interactions previously described for Ag-Ab complexes. The size of the Bet v 1 epitope is within the range defined by other complexes. Even though the existence of dominant IgE binding allergen epitopes is a matter of controversy, the concept is supported by the notion that natural exposure to surface patches conserved among structural homologues and isoallergens is higher and therefore more likely to induce high affinity IgE. The results of the IgE inhibition assays clearly suggest that dominant human IgE epitopes are located in conserved surface patches with the size of average Ag-Ab contact areas. These patches are therefore targets for modifications aiming at modulating the human allergen-specific immune response, with important implications for vaccine development. They also form the molecular basis of clinically observed cross-reactivity of tree pollen-allergic patients toward tree pollen allergens from related species.

## ► Acknowledgments

We thank Annette Giselsson and Gitte Bærentzen for expert technical assistance and Henning Løwenstein and Carsten Schou for valuable discussion.

## ► Footnotes

<sup>1</sup> This work was supported by the Danish Allergy Research Center (DARC) and the Danish Center for Synchrotron Radiation (DANSYNC). ■

<sup>2</sup> Current address, Department of Chemistry, Carlsberg Laboratory, Gamle Carlsbergvej 10, D-2500, Valby, Denmark. ■

<sup>3</sup> Address correspondence and reprint requests to Dr. Michael Gajhede, Protein Structure Group, Department of Chemistry, University of Copenhagen, Universitetsparken 5, DK-2100 Copenhagen Ø, Denmark. ■

<sup>4</sup> Abbreviations used in this paper: CDR, complementarity-determining region; RLU, relative light unit;

ncs, noncrystallographic symmetry; HMS, hot mean square deviation. ■

Received for publication June 21, 1999. Accepted for publication April 19, 2000.

## References

1. Holowka, D., B. Baird. 1996. Antigen-mediated IGE receptor aggregation and signaling: a window on cell surface structure and dynamics. *Annu. Rev. Biophys. Biomol. Struct.* 25:79. [Abstract]
2. Malissen, B.. 1998. Translating affinity into response [comment]. *Science* 281:528. [Full Text]
3. Gajhede, M., P. Osmark, F. M. Poulsen, H. Ipsen, J. N. Larsen, V. N. R. Joost, C. Schou, H. Lowenstein, M. D. Spangfort. 1996. X-ray and NMR structure of Bet v 1, the origin of birch pollen allergy. *Nat. Struct. Biol.* 3:1040. [Medline]
4. Ichikawa, S., H. Hatanaka, T. Yuuki, N. Iwamoto, S. Kojima, C. Nishiyama, K. Ogura, Y. Okumura, F. Inagaki. 1998. Solution structure of Der f 2, the major mite allergen for atopic diseases. *J. Biol. Chem.* 273:356. [Abstract/Full Text]
5. Mueller, G. A., D. C. Benjamin, G. S. Rule. 1998. Tertiary structure of the major house dust mite allergen Der p 2: sequential and structural homologies. *Biochemistry* 37:12707. [Medline]
6. Fedorov, A. A., T. Ball, R. Valenta, S. C. Almo. 1997. X-ray crystal structures of birch pollen profilin and Phl p 2. *Int. Arch. Allergy Immunol.* 113:109. [Medline]
7. Fedorov, A. A., T. Ball, N. M. Mahoney, R. Valenta, S. C. Almo. 1997. The molecular basis for allergen cross-reactivity: crystal structure and IgE-epitope mapping of birch pollen profilin. *Structure* 5:33. [Medline]
8. Rouvinen, J., J. Rautiainen, T. Virtanen, T. Zeiler, J. Kauppinen, A. Taivainen, R. Mantjarvi. 1999. Probing the molecular basis of allergy: three-dimensional structure of the bovine lipocalin allergen Bos d 2. *J. Biol. Chem.* 274:2337. [Abstract/Full Text]
9. Metzler, W. J., K. Valentine, M. Roebber, M. S. Friedrichs, D. G. Marsh, L. Mueller. 1992. Determination of the three-dimensional solution structure of ragweed allergen Amb t V by nuclear magnetic resonance spectroscopy. *Biochemistry* 31:5117. [Medline]
10. Paul, W.E.. 1999. Fundamental immunology: an introduction. *Fundamental Immunology* Lippincott-Raven, Philadelphia.
11. Momany, C., L. C. Kovari, A. J. Prongay, W. Keller, R. K. Gitti, B. M. Lee, A. E. Gorbalenya, L. Tong, J. McClure, L. S. Ehrlich, M. F. Summers, et al 1996. Crystal structure of dimeric HIV-1 capsid protein. *Nat. Struct. Biol.* 3:763. [Medline]
12. Padlan, E. A., E. W. Silverton, S. Sheriff, G. H. Cohen, S. J. Smith-Gill, D. R. Davies. 1989. Structure of an antibody-antigen complex: crystal structure of the HyHEL-10 Fab-lysozyme complex. *Proc. Natl. Acad. Sci. USA* 86:5938. [Medline]
13. Sheriff, S., E. W. Silverton, E. A. Padlan, G. H. Cohen, S. J. Smith-Gill, B. C. Finzel, D. R. Davies. 1987. Three-dimensional structure of an antibody-antigen complex. *Proc. Natl. Acad. Sci. USA* 84:8075. [Medline]
14. Chitarra, V., P. M. Alzari, G. A. Bentley, T. N. Bhat, J. L. Eisele, A. Houdusse, J. Lescar, H. Souchon, R. J. Poljak. 1993. Three-dimensional structure of a heteroclitic antigen-antibody cross-reaction complex. *Proc. Natl. Acad. Sci. USA* 90:7711. [Medline]
15. Lescar, J., M. Pellegrini, H. Souchon, D. Tello, R. J. Poljak, N. Peterson, M. Greene, P. M. Alzari. 1995. Crystal structure of a cross-reaction complex between Fab F9.13.7 and guinea fowl lysozyme. *J. Biol. Chem.* 270:18067. [Abstract/Full Text]

▲ [Top](#)  
 ▲ [Abstract](#)  
 ▲ [Introduction](#)  
 ▲ [Materials and Methods](#)  
 ▲ [Results and Discussion](#)  
 ▲ [References](#)

16. Ban, N., C. Escobar, R. Garcia, K. Hasel, J. Day, A. Greenwood, A. McPherson. 1994. Crystal structure of an idiotype-anti-idiotype Fab complex. *Proc. Natl. Acad. Sci. USA* 91:1604. [Abstract]
17. Colman, P. M., W. R. Tulip, J. N. Varghese, P. A. Tulloch, A. T. Baker, W. G. Laver, G. M. Air, R. G. Webster. 1989. Three-dimensional structures of influenza virus neuraminidase-antibody complexes. *Philos. Trans. R. Soc. London B Biol. Sci.* 323:511.
18. Malby, R. L., W. R. Tulip, V. R. Harley, J. L. McKimm-Breschkin, W. G. Laver, R. G. Webster, P. M. Colman. 1994. The structure of a complex between the NC10 antibody and influenza virus neuraminidase and comparison with the overlapping binding site of the NC41 antibody. *Structure* 2:733. [Medline]
19. Tulip, W. R., J. N. Varghese, W. G. Laver, R. G. Webster, P. M. Colman. 1992. Refined crystal structure of the influenza virus N9 neuraminidase-NC41 Fab complex. *J. Mol. Biol.* 227:122. [Medline]
20. Bossart-Whitaker, P., C. Y. Chang, J. Novotny, D. C. Benjamin, S. Sheriff. 1995. The crystal structure of the antibody N10-staphylococcal nuclease complex at 2.9 Å resolution. *J. Mol. Biol.* 253:559. [Medline]
21. Prasad, L., S. Sharma, M. Vandonselaar, J. W. Quail, J. S. Lee, E. B. Waygood, K. S. Wilson, Z. Dauter, L. T. Delbaere. 1993. Evaluation of mutagenesis for epitope mapping: structure of an antibody-protein antigen complex. *J. Biol. Chem.* 268:10705. [Abstract]
22. Li, H., J. J. Dunn, B. J. Luft, C. L. Lawson. 1997. Crystal structure of Lyme disease antigen outer surface protein A complexed with an Fab. *Proc. Natl. Acad. Sci. USA* 94:3584. [Abstract/Full Text]
23. Ipsen, H., O. C. Hansen. 1991. The NH2-terminal amino acid sequence of the immunochemically partial identical major allergens of alder (*Alnus glutinosa*) Aln g I, birch (*Betula verrucosa*) Bet v I, hornbeam (*Carpinus betulus*) Car b I and oak (*Quercus alba*) Que a I pollens. *Mol. Immunol.* 28:1279. [Medline]
24. Spangfort, M. D., H. Ipsen, S. H. Sparholt, S. Aasmul-Olsen, M. R. Larsen, E. Mortz, P. Roepstorff, J. N. Larsen. 1996. Characterization of purified recombinant Bet v 1 with authentic N-terminus, cloned in fusion with maltose-binding protein. *Protein Expression Purif.* 8:365.
25. Morrison, S. L.. 1999. Cloning, expression and modification of antibody V regions. , , , , ed. *Current Protocols in Immunology* Wiley, New York.
26. Spangfort, M. D., O. Mirza, L. A. Svensson, J. N. Larsen, M. Gajhede, H. Ipsen. 1999. Crystallization and preliminary X-ray analysis of birch pollen allergen Bet v 1 in complex with a murine monoclonal IgG Fab' fragment. *Acta Cryst.* 55:2035.
27. Otwinowski, Z.. 1993. Oscillation data reduction. *Proceedings of the CCP4 Study Weekend: Data Collection and Processing* 56. SERC Daresbury Laboratory, Warrington, U.K.
28. Navaza, J.. 1994. AMoRe: an automated package for molecular replacement. *Acta Cryst. A* 50:157.
29. Braden, B. C., H. Souchon, J. L. Eisele, G. A. Bentley, T. N. Bhat, J. Navaza, R. J. Poljak. 1994. Three-dimensional structures of the free and the antigen-complexed Fab from monoclonal anti-lysozyme antibody D44.1. *J. Mol. Biol.* 243:767. [Medline]
30. Brünger, A. T.. 1992. *X-PLOR Version 3.1: a System for X-ray Crystallography and NMR* Yale University Press, New Haven.
31. Lu, G., M. Villalba, M. R. Coscia, D. R. Hoffman, T. P. King. 1993. Sequence analysis and antigenic cross-reactivity of a venom allergen, antigen 5, from hornets, wasps, and yellow jackets. *J. Immunol.* 150:2823. [Abstract]
32. Jones, A., J. Y. Zou, S. W. Cowan, M. Kjeldgaard. 1991. Improved methods for building protein models in electron density maps and the location of errors in these maps. *Acta Cryst. A* 47:110.
33. Torigoe, C., J. K. Inman, H. Metzger. 1998. An unusual mechanism for ligand antagonism [comments]. *Science* 281:568. [Abstract/Full Text]
34. King, T. P., A. K. Sobotka, A. Alagon, L. Kochoumian, L. M. Lichtenstein. 1978. Protein allergens of white-faced hornet, yellow hornet, and yellow jacket venoms. *Biochemistry* 17:5165. [Medline]
35. Kungl, A. J., M. Susani, A. Lindemann, M. Machius, A. J. Visser, O. Scheiner, D. Kraft, M.

- Breitenbach, M. Auer. 1996. Evidence for an  $\alpha$  helical T cell epitope in the C-terminus of the main birch pollen allergen Bet V 1. *Biochem. Biophys. Res. Commun.* 223:187. [Medline]
36. Ipsen, H., J. N. Larsen. 1988. Detection of antigen specific IgE antibodies in sera from allergic patients by SDS-PAGE, immunoblotting and crossed radioimmuno-electrophoresis. , , ed. *Handbook of Immunoblotting of Proteins* 159. CRC Press, Boca Raton.
37. Harris, L. J., E. Skaletsky, A. McPherson. 1998. Crystallographic structure of an intact IgG1 monoclonal antibody. *J. Mol. Biol.* 275:861. [Medline]
38. MacCallum, R. M., A. C. Martin, J. M. Thornton. 1996. Antibody-antigen interactions: contact analysis and binding site topography. *J. Mol. Biol.* 262:732. [Medline]
39. Thorn, K. S., H. E. Christensen, R. Shigeta, D. Huddler, L. Shalaby, U. Lindberg, N. H. Chua, C. E. Schutt. 1997. The crystal structure of a major allergen from plants. *Structure* 5:19. [Medline]
40. Nicholls, A., K. A. Sharp, B. Honig. 1991. Protein folding and association: insights from the interfacial and thermodynamic properties of hydrocarbons. *Proteins* 11:281. [Medline]
41. Davies, D. R., E. A. Padlan, S. Sheriff. 1990. Antibody-antigen complexes. *Annu. Rev. Biochem.* 59:439. [Medline]
42. Schappi, G. F., C. Monn, B. Wuthrich, H. U. Wanner. 1996. Direct determination of allergens in ambient aerosols: methodological aspects. *Int. Arch. Allergy Immunol.* 110:364. [Medline]
43. Wahl, R., P. Schmid-Grendelmeier, O. Cromwell, B. Wuthrich. 1996. In vitro investigation of cross-reactivity between birch and ash pollen allergen extracts. *J. Allergy Clin. Immunol.* 98:99. [Medline]
44. Ebner, C., Z. Szepefalusi, F. Ferreira, A. Jilek, R. Valenta, P. Parronchi, E. Maggi, S. Romagnani, O. Scheiner, D. Kraft. 1993. Identification of multiple T cell epitopes on Bet v I, the major birch pollen allergen, using specific T cell clones and overlapping peptides. *J. Immunol.* 150:1047. [Abstract]

- ▶ [Abstract of this Article](#)
- ▶ [Reprint \(PDF\) Version of this Article](#)
- ▶ Similar articles found in:  
     [The JI](#)  
     [PubMed](#)
- ▶ [PubMed Citation](#)
- ▶ Search Medline for articles by:  
     [Mirza, O.](#) || [Gajhede, M.](#)
- ▶ Alert me when:  
     [new articles cite this article](#)
- ▶ [Download to Citation Manager](#)

HOME HELP FEEDBACK SUBSCRIPTIONS ARCHIVE SEARCH TABLE OF CONTENTS